Advances in
Science & Research
Open Access Proceedings

SATIN–Satellite driven nowcasting system

Ingo Meirold-Mautner, Alexander Kann, and Florian Meier

ZAMG – Zentralanstalt fü Meteorologie und Geodynamik, Department of forecasting models, Vienna, Austria

Correspondence to: Ingo Meirold-Mautner (ingo.meirold-mautner@zamg.ac.at)

Abstract. A precipitation nowcasting system (SATIN) is presented which relies entirely on satellite based precipitation products and rain gauge measurements. Thus, the proposed system is most suitable for areas where ground based radar observations are not available, or potentially suffer from low quality. SATIN delivers analyses on a 1 km grid every 15 min and nowcasts (obtained through motion vectors) in 15 min time steps. Nowcasts are gradually merged with NWP precipitation forecasts. An extensive validation including comparisons to different NWP models yields superior performance for SATIN analyses as well as nowcasts for lead times up to 1 h. Reducing the station density still yields better performance than operationally available NWP's.

1 Introduction

Satellite based observations play an important role in many different disciplines, such as meteorology, climatology, oceanography and many more. Specifically, derived precipitation estimates from space already deliver valuable information on a global scale. In regions with sparse ground based observation networks (rain gauge stations and ground based radars – simply referenced as "radar" in this paper), detailed knowledge about precipitation patterns and climatologies is largely missing and satellite observations are a key contributor for a better understanding of the regional weather and climate. Furthermore, regions with complex topography, where radar and station networks exist, may also profit from satellite observations, as radars suffer, among others, from beam blocking and usually only few station observations are available. Satellite based precipitation measurements could deliver additional information to mitigate the mentioned shortcomings.

The obtained precision of satellite based precipitation products is predominantly governed by the type of satellite orbit (polar orbiting, geostationary), instrument types (frequency bands used) and integration times (seasonal products to minutes). In this study we focus on nowcasting with very high temporal and spatial resolution, thus, the most challenging framework for satellite based precipitation products.

A prototype of a nowcasting system based on satellite precipitation in combination with rain gauge measurements (explicitly omitting radar observations) is developed. Such a system is of interest for data sparse regions where radar observations do not exist and rain gauge measurements are also scarce. Nevertheless, our target area is Austria where a dense observation network exists. This gives us the possibility of extensively validating the developed nowcasting system and comparing it to operationally available numerical weather prediction (NWP) models.

This satellite driven nowcasting system is based on the concepts of the INCA (Integrated Nowcasting through Comprehensive Analysis, Haiden et al., 2011) precipitation nowcasting and can be summarized as follows:

– Analyses are computed as a combination of rain gauge measurements and satellite derived precipitation. For each grid point, an average distance to neighboring stations enters the algorithm.

– Nowcasting is based on extrapolation by motion vectors computed from previous analyses.

– Very short range forecasting sets in after pure extrapolation: nowcasts are merged with precipitation forecasts from NWP through a prescribed weighting function until the forecasts entirely consist of downscaled NWP.

Results from long term validation and one case study are presented. Both yield good results for the analyses compared to operationally available NWP precipitation fields. Nowcastings deliver higher accuracy for lead times up to around

one hour compared to NWP forecasts. Additionally, sensitivity studies are presented to show the influence of station density on the results.

2   Data and methods

2.1   Target grid and NWP models

The target domain for the presented nowcasting system corresponds to the operational INCA domain in Austria. The grid spacing is $1\,\text{km} \times 1\,\text{km}$ with 700×401 grid points. By choosing this grid, validation of the results with INCA analyses becomes straightforward. Additionally, the following NWP models are used for comparisons and are interpolated onto the same grid: ALARO, AROME, AROME1km.

The ALARO model (Gerard and Geleyn, 2005) is a spectral limited area model (LAM) running four times per day operationally at ZAMG up to $+72\,\text{h}$ in hydrostatic mode with $4.8\,\text{km}$ horizontal grid spacing on a domain of 600×540 grid points covering Central Europe. It has 60 vertical hybrid levels (Simmons and Burridge, 1981) and its physics package 3MT is especially suitable for resolutions of few kilometers, where deep convection is only partly resolved.

Application of Research to Operations at Mesoscale (AROME) (Seity et al., 2011) is the second operational LAM at ZAMG running 8 times per day up to $+48\,\text{h}$ with a horizontal grid space of $2.5\,\text{km}$, 600×432 grid points and 90 hybrid levels in non-hydrostatic mode. Different to ALARO, deep convection is explicitly treated and the initial state of the atmosphere is generated by its own 3-D-Var data assimilation system (Brousseau et al., 2008). Both LAMs are coupled with the global model Integrated Forecasting System (IFS) of the European Centre for Medium-Range Weather Forecast (ECMWF) using Davies relaxation (Davies, 1976; Radnóti, 1995). For several test cases also a 1 km grid space version of AROME was run with a reduced time step (30 s instead of 60 s for AROME 2.5 km) on a domain of 800×500 grid points covering Austria and its surroundings with the same vertical resolution as AROME 2.5 km. It was coupled to and initialized by downscaled data from either IFS or ALARO 4.8 km or AROME 2.5 km.

2.2   Satellite data

Requirements to satellite data for precipitation nowcasting are high spatial and temporal resolution. To compete with radar based nowcastings, spatial resolution of a few kilometers and temporal resolution of a few minutes are necessary. Additionally, a low latency is required to ensure a rapid updating frequency and temporal availability of products.

Satellite products getting close to these requirements have been identified to be EUMETSAT's Support to Operational Hydrology and Water Management (H-SAF) and Support to Nowcasting and Very Short Range Forecasting (NWC SAF)

products as well as the HydroEstimator from NOAA. The products investigated are summarized in Table 1.

To determine the quality of the individual satellite products, a point validation against measurement stations and spatial validation against INCA analyses has been carried out (not shown in this study). While INCA analyses can not be considered to represent the truth (see Kann et al., 2015, for details on the quality of INCA precipitation analyses), they are the best option available for carrying out spatial comparisons. This validation included the computation of standard statistical scores (Root Mean Square Error RMSE, Bias) as well as objective verification measures (SAL, see Table 2). Both, point verification as well as spatial verification, indicate a consistent underestimation of satellite based precipitation, especially for the Convective Rainfall Rate (CRR) product (see Table 1 for details). Hydro-Estimator (HE) and H03 (precipitation product from HSAF) exhibit overall similar performance with lower biases for H03 but better representation of precipitation structures for HE (results from SAL verification, Wernli et al., 2008). As a consequence from these evaluations, the H03 product of HSAF was selected as input for SATIN as it shows best overall agreements with the reference and furthermore has the advantage of being available at 15 min temporal resolution (in contrast to 1 h for the HE product in Europe).

2.3   SATIN analysis

The SATIN analysis model is designed to take advantage from both constituent data sources: it combines the spatial characteristics of the precipitation patterns derived from satellite measurements with the accurate point measurements of the stations.

For a selected date/time combination, the developed system retrieves the corresponding satellite product from the HSAF data portal and interpolates the data to the INCA 1 km grid. This allows running SATIN for an arbitrary date/time combination (within the limits of availability of H03 data).

The second constituent of SATIN is precipitation measurements at stations. For the Austrian domain there are about 200 point observations from the "TeilAutomatisches Wetter ErfassungsSystem" (TAWES), equipped with tipping-bucket rain gauges, available. Processing of these station measurements corresponds to the algorithms developed for the operational INCA system. Besides aggregation to 15 min sums, station measurements are exposed to extensive quality control routines (Bica, 2012) in order to minimize the deterioration of nowcasting results through erroneous station measurements. These station observations are input to SATIN.

Once, all necessary input data for SATIN is collected and preprocessed, the combination algorithm with the following principal steps is launched:

–   At each grid point of the domain, an average distance t to the surrounding observation stations is computed.

Table 1. Overview of satellite products evaluated.

	H03	CRR	HE
Provider	Hydrology SAF	Nowcasting SAF	NOAA STAR
Spatial resolution	8 km	8 km	5 km
Temporal resolution	15 min	15 min	1 h (Europe)
Satellite	Meteosat (SEVIRI), LEO MW instrument (SSM/I, AMSU-A)	Meteosat (SEVIRI)	Meteosat (SEVIRI) (or others, e.g. GOES)
Characteristics	10.8 µm LUT, calibrated with MW LEO data	IR, VIS, WV channels, AUX data (NWP, etc.) for several correction algorithms	Single channel: 11 µm
Reference	Mugnai et al. (2013)	Rodríguez and Marcos (2014)	Scofield and Kuligowski (2003)

LEO: Low Earth Orbit; LUT: Look Up Table; MW: MicroWave; SAF: EUMETSAT Satellite Application Facility

Table 2. Statistical scores used in this study. See Wilks (2011) and Wernli et al. (2008) for details.

	FBI	TSS	ETS	SAL		
Name	Frequency Bias Index	True Skill Score	Equitable Threat Score	Structure	Amplitude	Location
Range	$0-\infty$	$-1-1$	$-1/3-1$	$-2-2$	$-2-2$	$0-2$
Perfect	1	1	1	0	0	0
Characteristic	How did the forecast frequency of "yes" events compare to the observed frequency of "yes" events?	How well did the forecast separate the "yes" events from the "no" events?	How well did the forecast "yes" events correspond to the observed "yes" events?	Positive if cells are too large and/or too flat	Relative deviation of domain averaged precipitation	Displacement of precipitation cells
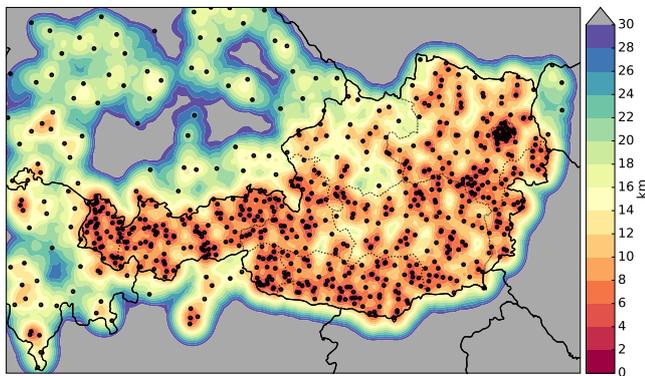
Figure 1. This figure depicts the SATIN domain (same as INCA operational domain). Black dots represent automatic weather stations entering the SATIN algorithm. Average distance for three nearest neighbors is shown (with a cutoff at distances larger than 30 km).

This is done by searching for N nearest neighbors and averaging the obtained distances. Tests have been made with different numbers of nearest neighbours to include in the computation. Small numbers yield a larger variability in the average distance and thus lead to more granularity regarding the influence of satellite data on the SATIN analysis. $N = 3$ (as depicted in Fig. 1) was chosen for this study as it gives more weight to satellite data in areas with smaller station density and shows a pronounced granularity in the transition from station to satellite derived precipitation, when compared to larger values of N. This step is redone for each time step because station density is varying.

– Station observations are interpolated to the INCA grid by inverse distance weighting (IDW) of the 8 nearest neighbor stations to each grid point. Weights are computed proportional to $1/d^2$, i.e. with decreasing weights for increasing distance d. This results in the station precipitation field RR_{STAT}.

– Weighting factors at each grid point for merging satellite data with station data are computed. This weighting factor is computed from a logistic function which describes the transition from station to satellite data: $w = 1/(1 + \exp(-k(t - u)))$. The above computed average distance enters the logistic function as t. Equal weights to satellite and station are attributed at an average distance of $u = 30$ km. The parameter k (set to 0.2) determines the steepness of the function, i.e. the rate at which weights are changing with distance. Experiments with different parameters of the logistic function have been performed, with the above described setting found to provide a good balance between station measurements and satellite precipitation for the characteristics of the Austrian domain. The weighting factor as a function of distance is plotted in Fig. 2.
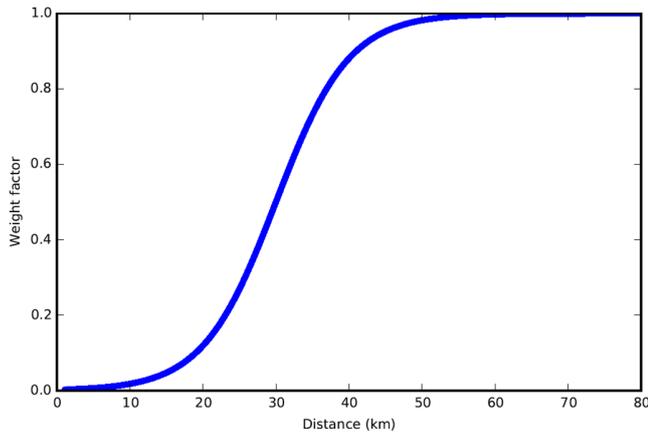
Figure 2. Weights w computed as a logistic function and plotted against distance d. Parameters of the logistic function are described in the text.

– The final precipitation rate based on satellite and station at each grid point is then obtained by $RR_{\text{SATIN}} = wRR_{\text{SAT}} + (1-w) \times RR_{\text{STAT}}$, where RR_{SAT} denotes the preprocessed satellite precipitation.

The described algorithm is thus taking the satellite derived precipitation product and merges this with the interpolated station observations. Depending on average station density, more weight is either given to the satellite product or the station observations. In regions with very sparse station density, the SATIN analysis will therefore resemble the raw satellite precipitation product, whereas regions with high station density will benefit from accurate point measurements. Figure 1 shows the average distance computed with three nearest neighbors. Including more nearest neighbors in the computation results in a smoother spatial distribution of the weight factor (not shown). Figure 2 depicts the weight factor as a function of average distance which indicates that grid points within an average distance of around 20 km are mostly influenced by station measurements. Beyond this distance, the influence of satellite precipitation is rapidly increasing.

The SATIN analysis and nowcasting model is coded in Python with a modular approach. A pre-processing module is responsible for fetching necessary satellite products and interpolating them to the target grid. Some functionalities are taken directly from the operational INCA model, such as the computationally demanding motion vector estimation, and the quality filtering of station measurements.

2.4   SATIN nowcasting

Pure nowcasting is based on motion vectors computed from previous satellite precipitation fields. The same cross correlation algorithm as the one in INCA is applied (see Haiden et al., 2011) to obtain the motion vectors. However, no cross-checking with upper air flow from NWP output is done (as

opposed to the INCA algorithm). This decision is made in order to stay independent of NWP input. The resulting motion vectors are however less stable and spurious correlations exist, which introduces errors in the translational nowcasting. In order to minimize the deterioration of the relatively good SATIN analyses, the translational motion is obtained from averaging the motion vectors.

Beyond the pure nowcasting, merging with NWP is applied. This is done to benefit from the different strengths of each forecasting system, the observation based nowcasting for very short time ranges and the physically based NWP for longer time ranges. Finding the optimal transition from nowcasting to NWP amounts to identifying when NWP yields superior results than pure nowcasting. Varying results are expected, especially when looking at rather convective weather types opposed to stratiform precipitation events.

To investigate the characteristics of NWP and nowcasting performances for both types of precipitation (convective and stratiform), scores have been computed for one winter month (January 2014) and one summer month (July 2014) with INCA analyses serving as reference. Figure 3 shows relative RMSE, MAE (Mean Absolute Error) and Bias while Fig. 4 shows the skill scores FBI, TSS and ETS (for a threshold of $1\,\text{mm}\,15\,\text{min}^{-1}$) averaged for July (cf. to Table 2 and e.g. Wilks, 2011, regarding skill scores). Rather than discussing in detail the individual scores (which all suffer from weaknesses, such as double-counting penalty), it is important to note the variation with lead time. Average RMSE, MAE and Bias for the NWP's remain almost constant for lead times up to 6 h, with ALARO exhibiting a better performance than AROME except for bias in the convective season. SATIN performance is very good for very short lead times and decreases rapidly with increasing lead times. RMSE and MAE of ALARO reach similar values to SATIN for lead times between 30 min and 1 h (for July and January, respectively). A similar picture arises for the skill scores in Fig. 4 where lead times of roughly 1 h mark the time when NWP outperforms the SATIN nowcasting. In this paper only results from July are shown as the results from January reveal a similar behavior with better performance of SATIN in the first hour of forecasts. In January the error levels are generally smaller for all models (SATIN, ALARO, AROME), which indicates a better performance in the non-convective season.

3   Validation of SATIN and comparison to NWP

3.1   Validation of SATIN analysis

The SATIN algorithm strives to obtain an optimal combination of satellite data and station observations to provide precipitation analyses. In this section the SATIN analyses are compared to the pure satellite product that serves as input to SATIN as well as to the currently operational local area NWP at ZAMG (ALARO5).
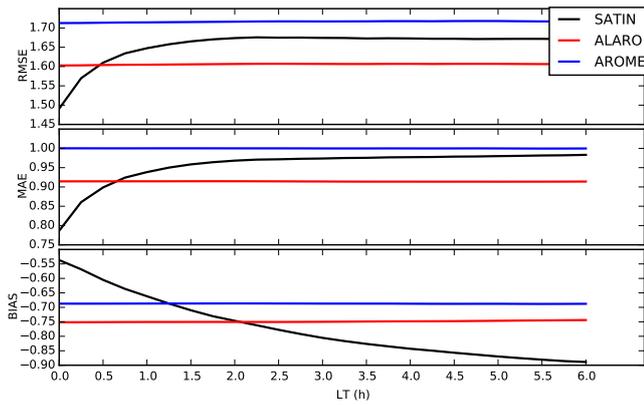
Figure 3. Comparison of pure (translational) nowcasting with NWP: relative RMSE, MAE and Bias averaged over July for ALARO (5 km), AROME (2.5 km) and SATIN.
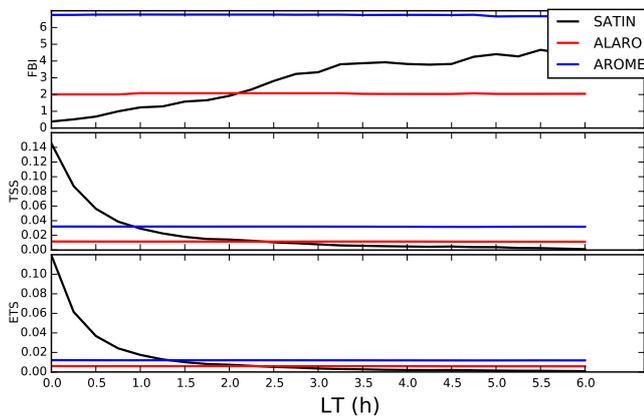
Figure 4. Comparison of pure (translational) nowcasting with NWP: FBI, TSS and ETS averaged over July for ALARO (5 km), AROME (2.5 km) and SATIN.

For the comparison with SATIN analyses, NWP output is taken as it would be available in an operational environment (i.e. at a given SATIN analysis time an NWP analysis is not available, thus an NWP forecast valid for this time has to be taken for comparison purposes.). Reference in these comparisons are the INCA precipitation analyses. At 5 selected days with heavy precipitation, standard verification measures RMSE, MAE, Bias as well as the objective SAL verification has been carried out. Figure 5 represents the SAL result. It can be seen from this figure, that SATIN analyses significantly reduce the spread in the data and have narrower distributions than the satellite and NWP products. Structure and Location are very well represented by SATIN in most cases. The results for Amplitude exhibit much lower spread as e.g. in the NWP output, however the mean values of NWP sometimes yield better results than those of SATIN.

Additionally to the case studies of the previous comparisons, statistics have been computed for two months, one in winter and one in summer. SATIN has been computed with 9
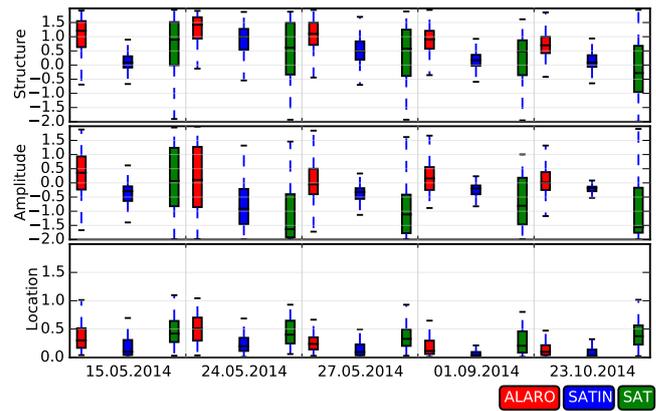
Figure 5. Validation of SATIN analyses with INCA analyses and comparison to ALARO and H03 (SAT) satellite precipitation product. Box plots of daily Structure, Amplitude, Location values for 5 cases with heavy precipitation.

Table 3. Mean relative RMSE, MAE and Bias obtained from cross validation at 9 stations for January and July 2014. NWP refers to ALARO 5 km while SAT refers to the HSAF H03 product.

| | January | | | July | | |
	NWP	SAT	SATIN	NWP	SAT	SATIN
RMSE	0.86	1.12	0.71	1.26	1.58	0.99
MAE	0.72	0.99	0.60	0.89	1.19	0.64
Bias	−0.52	−0.87	−0.45	−0.76	−0.39	−0.35

TAWES stations not entering the algorithm (see Fig. 6). By excluding these stations, a cross validation can be carried out by computing statistics at these exact stations. For comparison, SAT (H03) and NWP (ALARO5) are also investigated and compared to SATIN. Relative RMSE, MAE and Bias are averaged over the summer and winter months and the results for January and July 2014 are shown in Table 3.

SATIN clearly outperforms both, ALARO5 and H03 in all standard verification parameters. Specifically, the bias during the convective season in July 2014 is much smaller in SATIN than in the NWP fields.

3.2 Nowcasting compared to NWP

At lead times beyond the pure nowcasting range, the SATIN system is blended with an NWP model. This is done because pure nowcasting (shifting of cells according to motion vectors) does not include any dynamical or physical aspects (as in NWP's) and thus is not able to describe the future state of the atmosphere for lead times larger than a couple of hours. The combination of pure nowcasting and NWP provides the advantage of merging current observations and derived nowcasts with physically based NWP models. It is crucial to determine the optimal timing for switching from one system
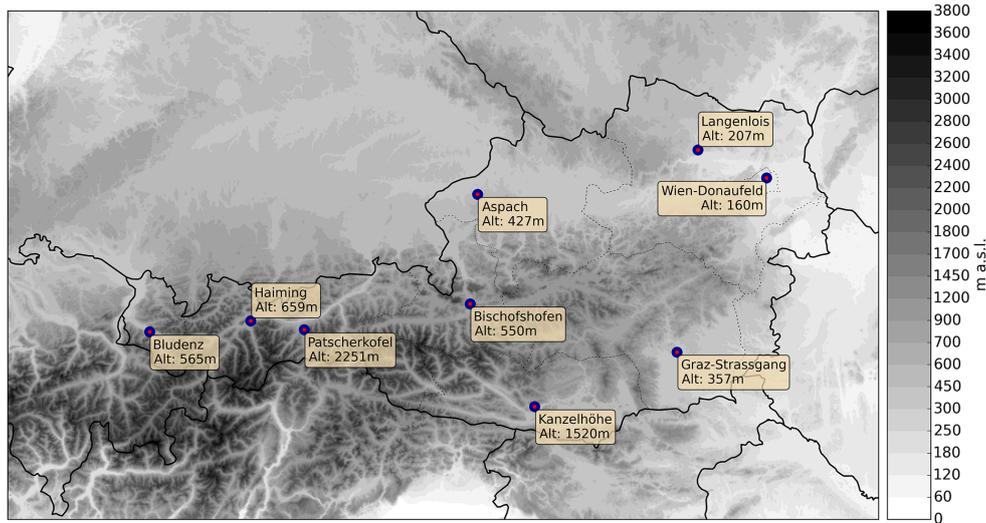
Figure 6. INCA domain and topography. Information on excluded TAWES stations for cross validation of SATIN analyses is included.

(nowcasting) to the other (NWP) in order to optimally profit from the advantages of both systems.

A transition phase marks the lead times where the different models, nowcasting and NWP, are combined. Before the transition phase, SATIN consists of pure nowcasting, after the transition phase SATIN is governed by NWP exclusively. Within the transition phase the weights of the NWP model are gradually increased while the contributions from pure nowcasting are decreased. Therefore, at lead times beyond the transition phase, the SATIN system entirely relies on the NWP model output, delivering the forecasts interpolated on the 1km INCA grid.

Deciding which NWP model should be used for the blending with nowcasting is not an easy task, as each of the available models has its strengths and weaknesses. Rather than evaluating the NWP models (which is beyond the scope of this study), we compare several models to pure nowcasting.

The NWP models investigated are ALARO (5 km), AROME (2.5 km) and AROME (1 km). For the same cases as in Fig. 5, daily average error scores (RMSE, MAE, Bias, SAL, FBI, TSS, ETS) are computed and plotted as a function of the lead time. The resulting scores are then averaged (over the cases) to obtain Figs. 7–9.

Relative RMSE, MAE and Bias in Fig. 7 show for pure nowcasting (SATIN) a clear increase of error with increasing lead time. At analysis time, the error measures are all below the values obtained from the different NWP models. Relative RMSE and MAE reach the level of ALARO (best performing NWP for the selected cases) after about 1h lead time. Relative Bias of SATIN becomes larger than the one of AROME (2.5 km) after less than 30 min lead time.

Objective verification measures Structure, Amplitude and Location as shown in Fig. 8 exhibit much less dependency on lead times. Only the Location measure shows an increase
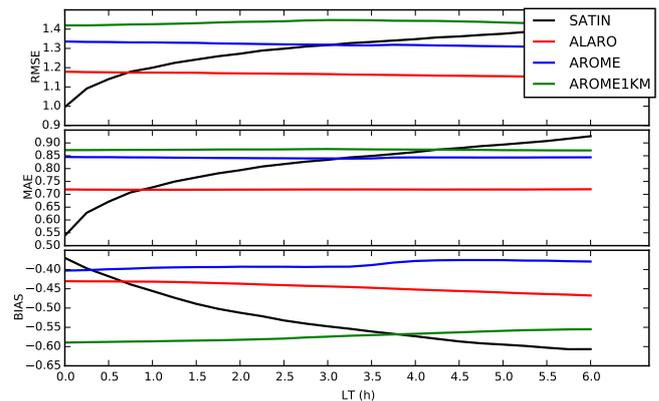
Figure 7. Comparison of pure (translational) nowcasting with NWP models: relative RMSE, MAE and Bias versus lead time, averaged over five days with heavy precipitation.

for SATIN with lead time and reaches values as those from the NWP's at around 1.5 to 2 h lead time. This suggests, that localisation of precipitation cells are very well captured in the analysis but the translational motion in pure nowcasting rapidly deteriorates the result. In contrast NWP Location values are almost constant over lead time. As was already noted in Sect. 2.4, the computation of motion vectors can lead to unrealistic translational movement of cells and needs further optimisation and revision which is beyond the possibilities of this project.

Amplitude and Structure values of SATIN remain relatively constant with lead time and show similar values as AROME (1 km) and AROME (2.5 km) respectively. The results for Amplitude and relative Bias do not match exactly, with positive Amplitude values for ALARO and AROME (2.5 km) and negative relative Bias of the same models.
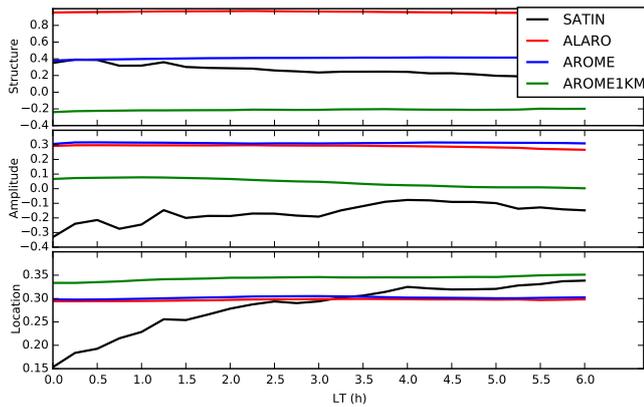
Figure 8. Comparison of pure (translational) nowcasting with NWP models: Structure, Amplitude, Location versus lead time, averaged over five days with heavy precipitation.

Figure 9. Comparison of pure (translational) nowcasting with NWP models: FBI, TSS, ETS versus lead time, averaged over five days with heavy precipitation.

Structure is best represented by SATIN and the AROME model in 2.5 km resolution. ALARO (5 km) is overestimating Structure while AROME (1 km) is underestimating this parameter. Thus, ALARO tends to overestimate the extent of precipitation fields and AROME (1km) tends to underestimate them – compared to INCA analyses.

Skill scores FBI, TSS and ETS, as depicted in Fig. 9, show again a dependency on lead time for SATIN. Results for the NWP models are relatively constant. The scores for SATIN yield better results than NWP models for lead times below about 1.5 h. The bias related index FBI for the NWP's shows best results for ALARO and worst results for AROME (1 km). This again indicates the different characteristics of the scores (Bias, Amplitude and FBI). Scores were computed for a threshold of 1 mm 15 min^{-1}.

The presented results are based on a few heavy precipitation cases and may not be representative for low impact situations. Nevertheless, they give an impression of what can be expected from a satellite based nowcasting system. Analyses tend to give excellent results, with a pronounced decrease in performance for increasing lead times. According to these results, transition from pure nowcasting to NWP's should take place somewhere between 30 min and 2 h. As the investigated scores show quite different behavior, it is not easy to exactly determine the best transition time exactly, but rather depend on the scale of interest, the weather type and the application.

3.3 Sensitivity to station density

In Austria (and most European countries), the density of automatic weather stations of different providers (e.g. national meteorological services, hydrological services, etc.) for precipitation measurements is relatively high, with a mean distance between neighbouring stations of about 12 km, or roughly 700 stations. However, in many regions of the world, where a satellite based precipitation nowcasting would be most beneficial (due to the absence of radar), station density
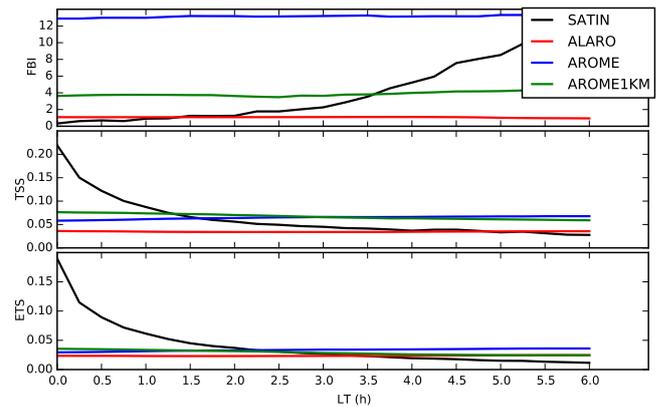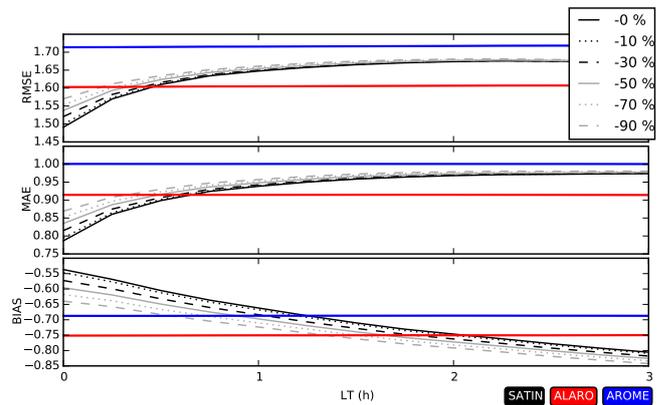
Figure 10. Relative RMSE, MAE and Bias per lead time (LT) averaged over July 2014. Several SATIN runs are shown with progressively less stations entering the algorithm. ALARO and AROME are shown as reference.

is much lower. Therefore, the influence of station density on the skill of the analysis is quite important to estimate the benefit of such a system in data sparse regions.

Experiments have been run to investigate the effect of reduced station density on the SATIN nowcasting performance and consequently on the optimal transition time to NWP model output. For each of the experiments an increasing amount of stations measuring non-zero precipitation has been selected and excluded from the SATIN nowcasting computation. SATIN runs were performed for 10, 30, 50, 70 and 90 % of stations missing. Results are averaged over July 2014 and are shown in Fig. 10. Reducing the station density by half (50 %) shows for RMSE and MAE around half of the original (no stations excluded) lead time as optimal transition time. For the analysis, a 10 % increase of the error measures can be observed when comparing 90 % excluded stations with standard SATIN runs. These results suggest, that in regions with very low station density, an anal-
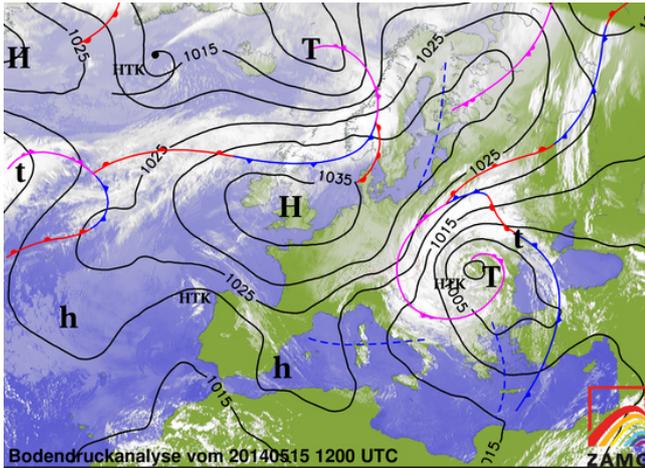
Figure 11. Satellite image (MSG IR), surface pressure analysis and frontal zones for 15 May 2014 at 12:00 UTC.
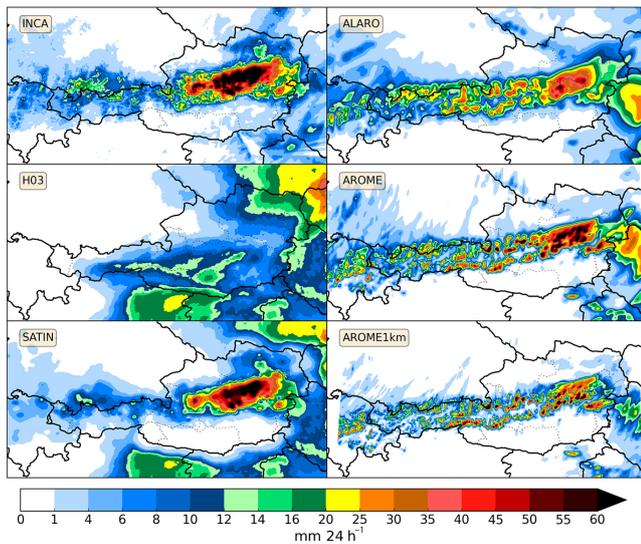
Figure 12. 24 h precipitation sum from different models for 15 May 2014.

Figure 13. Comparison of pure (translational) nowcasting with NWP models on 15 May 2014: relative RMSE, MAE and Bias of forecasts per LT.
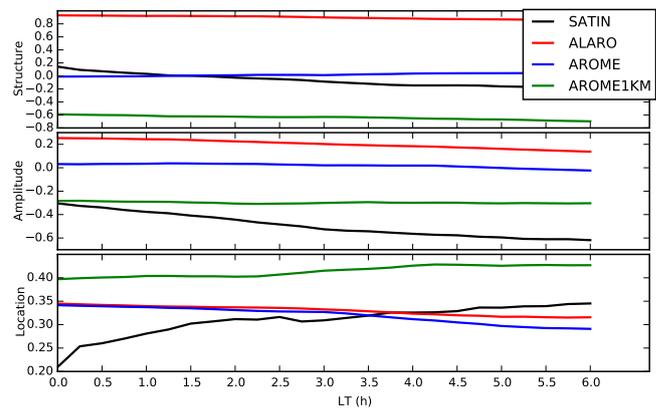
Figure 14. Comparison of pure (translational) nowcasting with NWP models on 15 May 2014: Structure, Amplitude and Location of forecasts per LT.

ysis and nowcasting system as proposed in this study, still yields better results than NWP models for the analysis and lead times of up to 30 min. Low station density will not only affect a poorer nowcasting quality but also poorer NWP performance, thus the quality of NWP forecasts will also deteriorate.

3.4   Case study – 15 May 2014

The synoptic situation is characterised as a high pressure system over the British Isles and a low pressure system over Romania with a cold air flow from the north reaching Austria. On the backside of this low pressure system, intensive precipitation is observed which is accompanied by strong north-westerly winds. The center of the low pressure system is gradually moving westwards which leads to increasing precipitation rates across the Alps. Heavy precipitation is mostly centred over the eastern parts of the domain (Figs. 11 and 12).

Average scores per lead time are computed for each forecast and plotted in Figs. 13 and 14. Results on this day clearly show the superior performance of SATIN (in pure translation mode without model merging) compared to the other models for lead times up to 1 h. At longer lead times the SATIN result deteriorates and gradually drops below the worst NWP results (in this case AROME 1 km). For this case a gradual merging of SATIN with ALARO gives best results. This is also the principal configuration chosen in the SATIN system. The good performance of SATIN for this case can certainly be attributed to the measurement stations, as the H03 product almost completely misses the heavy precipitation (compare Fig. 12).

4 Conclusions

The satellite based nowcasting system SATIN yields more accurate analysis fields compared to operationally available NWP forecasts. This finding also holds when the rain gauge station density is artificially reduced significantly.

Pure translational nowcasting with SATIN yields better scores than NWP forecasts for lead teams of around 1 h. Results indicate, that a transition from pure nowcasting to NWP should take place between 1 and 2 h.

A simple approach of merging station observations with satellite precipitation has been applied. As satellite precipitation products occasionally suffer from massive underestimation of precipitation and generally exhibit quite varying performance, a more sophisticated merging algorithm might improve the analysis (e.g. Kriging methods).

The computation of motion vectors can lead to unrealistic results and needs further improvement. Possibly, other methods of computing translational motion should be investigated (e.g. use of atmospheric motion vectors from nowcasting SAF, or implementing other concepts such as optical flow).

Nevertheless, the presented system is a simple and robust method for obtaining accurate analyses and nowcasts in the absence of radars. Besides possible improvements to the current system with the mentioned techniques, further studies could investigate on the combination with radar data, or the implementation of the system in data sparse regions.

References

Bica, B.: Filter algorithms in the INCA precipitation analysis, Technical Report, ZAMG, 1–2, 2012.

Brousseau, P., Bouttier, F., Hello, G., Seity, Y., Fischer, C., Berre, L., Montmerle, T., Auger, L., and Malardel, S.: A prototype convective-scale data assimilation system for operation: the Arome-RUC, HIRLAM Techn. Report, 68, 23–30, 2008.

Davies, H.: A lateral boundary formulation for multi-level prediction models, Q. J. Roy. Meteor. Soc., 102, 405–418, 1976.

Gerard, L. and Geleyn, J.-F.: Evolution of a subgrid deep convection parametrization in a limited-area model with increasing resolution, Q. J. Roy. Meteor. Soc., 131, 2293–2312, 2005.

Haiden, T., Kann, A., Wittmann, C., Pistotnik, G., Bica, B., and Gruber, C.: The Integrated Nowcasting through Comprehensive Analysis (INCA) system and its validation over the Eastern Alpine region, Weather Forecast., 26, 166–183, 2011.

Kann, A., Meirold-Mautner, I., Schmid, F., Kirchengast, G., Fuchsberger, J., Meyer, V., Tüchler, L., and Bica, B.: Evaluation of high-resolution precipitation analyses using a dense station network, Hydrol. Earth Syst. Sci., 19, 1547–1559, doi:10.5194/hess-19-1547-2015, 2015.

Mugnai, A., Casella, D., Cattani, E., Dietrich, S., Laviola, S., Levizzani, V., Panegrossi, G., Petracca, M., Sanò, P., Di Paola, F., Biron, D., De Leonibus, L., Melfi, D., Rosci, P., Vocino, A., Zauli, F., Pagliara, P., Puca, S., Rinollo, A., Milani, L., Porcù, F., and Gattari, F.: Precipitation products from the hydrology SAF, Nat. Hazards Earth Syst. Sci., 13, 1959–1981, doi:10.5194/nhess-13-1959-2013, 2013.

Radnóti, G.: Comments on "A spectral limited-area formulation with time-dependent boundary conditions applied to the shallow-water equations", Mon. Weather Rev., 123, 3122–3123, 1995.

Rodríguez, A. and Marcos, C.: Product User Manual for the "Convective Rainfall Rate" (CRR – PGE05 v4.0), Techn. Rep., NWC-SAF, http://www.nwcsaf.org/, 2014.

Scofield, R. A. and Kuligowski, R. J.: Status and outlook of operational satellite precipitation algorithms for extreme-precipitation events, Weather Forecast., 18, 1037–1051, 2003.

Seity, Y., Brousseau, P., Malardel, S., Hello, G., Bénard, P., Bouttier, F., Lac, C., and Masson, V.: The AROME-France convective-scale operational model, Mon. Weather Rev., 139, 976–991, 2011.

Simmons, A. J. and Burridge, D. M.: An energy and angular-momentum conserving vertical finite-difference scheme and hybrid vertical coordinates, Mon. Weather Rev., 109, 758–766, 1981.

Wernli, H., Paulat, M., Hagen, M., and Frei, C.: SAL–A novel quality measure for the verification of quantitative precipitation forecasts, Mon. Weather Rev., 136, 4470–4487, 2008.

Wilks, D. S.: Statistical methods in the atmospheric sciences, vol. 100, Academic press, 2011.